Running Safety of Vehicle on the Bridge under the Sudden Change of Wind Loads Due to Wind Barriers

Xin-yu Xu and Xiao-long Zheng
China Railway Eryuan Engineering Group Co., Ltd, Chengdu, China
Email: lsxxy90@126.com

Yong-le Li
Southwest Jiaotong University, Chengdu, China

***Abstract*—Wind barriers are the efficient and simplest devices for the wind protection of vehicle. To investigate the dynamic responses of vehicle passes through the transition section of wind barriers, a high-speed railway simply-supported beam bridge was taken as the research object. Aerodynamic characteristics of vehicle-bridge system were tested in wind tunnel tests, and the effects of wind barrier porosities were considered. The wind-vehicle-bridge (WVB) coupling analysis was conducted by Dummy Body Coupling (DBC) method. The results show that dynamic responses of the vehicle generally tend to increase with the increase in speed. In the wind barrier section, the dynamic responses would decrease, accounting for the wind shielding effects. The lateral and vertical accelerations are sensitive to the sudden changes of wind loads due to the wind barrier, while the lateral force and reduction rate of wheel load have little sudden change when the vehicle enters and leaves the wind barrier section.**

***Index Terms*—wind-vehicle-bridge system, coupling vibration, wind barriers, sudden change of wind loads, aerodynamic characteristics**

I. Introduction

Strong crosswind is a vital problem for securing the safety of vehicles, and accidents posed by wind gusts on vehicles passing through the bridges have been reported around the world, which attracts increasing attention [1-3].

Presently, to ensure the running safety of vehicle on the bridge under strong wind, setting wind barriers on the bridge has become a preference for the wind protection of vehicle. Current research mainly focuses on the protection effects, and investigate the distributions of the wind field behind the wind barriers, aerodynamic characteristics and dynamic responses of vehicle further.

Chu et al. compared the results of Computational Fluid Dynamics (CFD) and wind tunnel test and verified the CFD method, calculated the wind loads on the vehicle with wind barriers and evaluated the protection effects [4]. Ogueta-Gutiérrez et al. investigated the effects of different types of wind barrier on aerodynamic characteristics of bridge and vehicle by wind tunnel tests [5]. Xiang et al. studied the effects of wind barriers on aerodynamic characteristics of moving vehicle under different wind yaw angle and the aerodynamic interactions between vehicles and wind barriers on a railway bridge [6-7].

Previous research is mostly about the comparison of protection effects of wind barriers. Under the perspective of saving the engineering and improving the efficiency of utilizing the wind barriers, the wind barriers are not suitable for setting on the whole railway line. Hence, it should be proper to setting the wind barriers in the strong wind area, via the historical information survey or wind field test along the rail line. However, the sudden wind effects are bought about when vehicle enters and leaves the wind barrier section under the strong wind circumstance, which maybe causes the unfavorable influences.

To study the running safety of vehicle on the bridge under the sudden change of vehicle wind loads due to wind barriers, a high-speed railway simply-supported beam bridge was taken as the research object, the dynamic responses of whole process of vehicles entering and leaving the wind barrier section under the strong wind circumstance were simulated, by wind-vehicle-bridge (WVB) coupling vibration method.

II. Modeling of Wind-Vehicle-Bridge System

A. Wind

Wind velocity fluctuation is one of excitations for the WVB system, and the velocity fields are simulated as stationary Gaussian stochastic processes using spectral representation method. In this study, static wind loads and buffeting loads on both vehicle and bridge are considered.

Static wind loads on vehicle and bridge deck in unit length can be expressed as follows:

Manuscript received March 14, 2018; revised March 12, 2019.
Project number: National Key R&D Program of China (2017YFB1201204).

doi: 10.18178/ijscer.8.2.165-170

$$D_{st} = \frac{1}{2}\rho \overline{U}^2 H C_D \quad (1)$$

$$L_{st} = \frac{1}{2}\rho \overline{U}^2 B C_L \quad (2)$$

$$M_{st} = \frac{1}{2}\rho \overline{U}^2 B^2 C_M \quad (3)$$

where D_{st}, L_{st} and M_{st} are the drag force, the lift force and the moment, respectively; ρ is the air density; $\overline{U}$ is the upstream mean wind velocity; C_D, C_L and C_M are the drag coefficient, the lift coefficient and the moment coefficient, respectively; H and B are the height and the width of the vehicle or the bridge deck.

Three-component forces on bridge and vehicle are shown in Fig. 1.

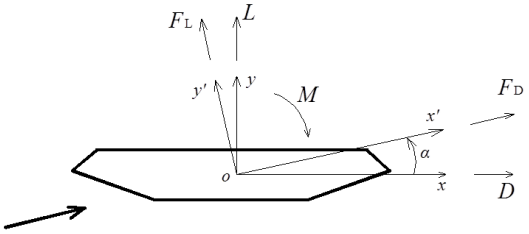

(a) Bridge

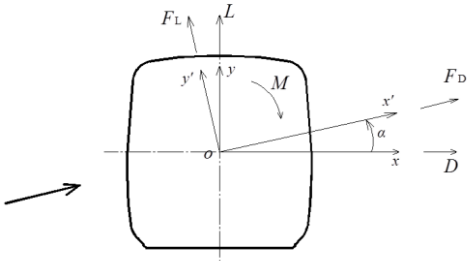

(b) Vehicle

Figure 1. Three-component forces on bridge and vehicle.

Buffeting loads are induced by stochastic wind fluctuations. According to the quasi-steady theory, and aerodynamic admittance functions (ADF) are introduced to correct the wind loads. In reference to the existed study, the cosine rule can be approximately used to determinate wind loads, and buffeting loads on the deck or the vehicle in unit length can be expressed as follows [8-9]:

$$D_{bu} = \frac{1}{2}\rho \overline{U}^2 B\left[2C_D \chi_{Du}\frac{u(t)}{\overline{U}} + C_D' \chi_{Dw}\frac{w(t)}{\overline{U}}\right] \quad (4)$$

$$L_{bu} = \frac{1}{2}\rho \overline{U}^2 B\left\{2C_L \chi_{Lu}\frac{u(t)}{\overline{U}} + [C_L' + C_D]\chi_{Lw}\frac{w(t)}{\overline{U}}\right\} \quad (5)$$

$$M_{bu} = \frac{1}{2}\rho \overline{U}^2 B^2\left\{2C_M \chi_{Mu}\frac{u(t)}{\overline{U}} + C_M' \chi_{Mw}\frac{w(t)}{\overline{U}}\right\} \quad (6)$$

where $C_L^{'}$, $C_L^{'}$ and $C_M^{'}$ are the slopes of C_D, C_L and C_M, respectively; γ_i (i = 1, 2, ... , 5) are the aerodynamic admittance functions, and χ is the values of admittance function, approximately taken as 1.0 in this study; $u(t)$ and $w(t)$ are the wind velocity fluctuation in the wind flow direction and the vertical direction, respectively.

B. Train Model

The train is a complicated multi-degree-of-freedom (multi-DOF) spatial vibration system, of which the vibration is categorized into the lateral, longitudinal, vertical, yaw, pitch and roll motions. A high-speed train fundamentally consists of car bodies, bogies and wheelsets, which are defined by the body in the MBS. A schematic model of a train is shown in Fig. 2. In this paper, the CRH (China Railways High-speed) train model was established.

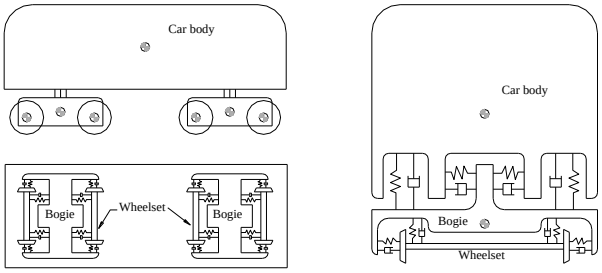

Figure 2. Schematic model of a train.

C. Bridge Model

The bridge models are established using the FE method, and then introduced into the MBS software as the elastic body by substructure analysis. In the study, commercial software ANSYS was adopted for the structural analysis.

The WVB system based on the Dummy Body Coupling (DBC) method (Fig. 3) is regarded as a united and coupled system, and the equations of motion of the whole system are solved directly [10-11].

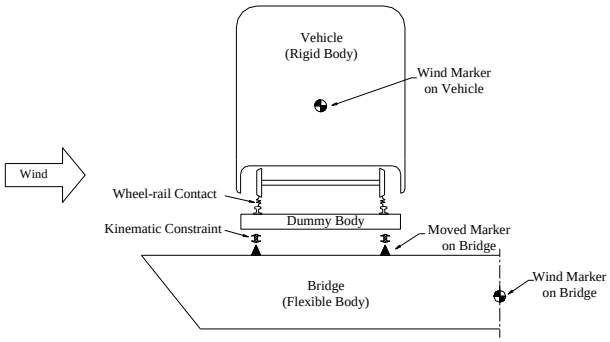

Figure 3. WVB model based on the DBC method.

III. Engineering Description and Wind Loads

A. Engineering Background

A 20×32m high-speed railway simply-supported beam bridge was taken as the research object. The transverse distance between the track lines is 5 m. Finite element model of the bridge was established using ANSYS software, where main beam and piers were simulated by spatial beam element (seeing Fig. 4).

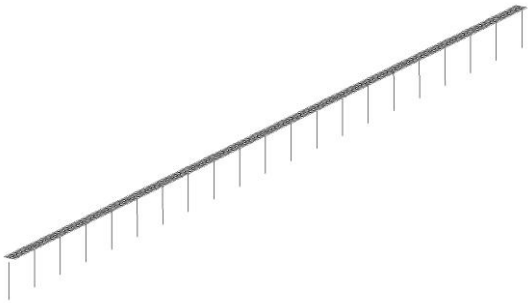

Figure 4. Finite element model of bridge.

The track irregularities were generated according to the power spectrum density function of the German low-disturbance track spectrum, of which the alignment, vertical-profile and cross-level irregularities were considered. Damping ratio of the bridge was taken as 2%.

B. Aerodynamic Characterictics

As the wind loads on the windward vehicles are generally larger than those on the leeward vehicle, the vehicle was positioned at the windward side in the following discussion. In the study, three types of wind barriers were adopted, including 3.5m high wind barriers of 100% (no wind barriers), 43.5% and 0%(solid) porosity. The vehicle-bridge section model test was conducted in the wind tunnel [12]. Static aerodynamic coefficients of the vehicle are listed in Table 1, noting that the mutual interferences between the vehicle and the deck are considered.

TABLE I. AERODYNAMIC COEFFICIENTS OF VEHICLE

Porosity	C_D	C_L	C_M
100%	1.710	0.739	-0.098
43.5%	1.082	0.554	-0.089
0%	0.2300	-0.0242	0.0173

C. Wind Velocity Fields

The incoming wind mean velocity was taken as $\overline{U}$ = 20 m/s, and the wind acted perpendicularly to the vehicle advancing direction. The velocity fields are simulated as stationary Gaussian stochastic processes using spectral representation method. In total, 81 wind velocity fluctuation simulation points were positioned along the 20-span bridge, and the space between two points was 8m.

Based on the fixed-point spectrum simulation, the wind velocity fluctuation in the wind flow direction at the discrete locations was calculated. When the vehicles operate along the wind field points at a certain speed, the time history of wind velocity on one point of the vehicle is a spatiotemporal distribution function corresponding with the vehicle speed. When the vehicle arrives at one wind velocity discrete point *P*, the wind velocity fluctuation acting on the moving vehicle at the *t* time is the wind velocity fluctuation at the *t* time of the discrete point *P*. Hence, the time history of wind velocity fluctuation on the moving vehicle can be obtained from the discrete wind field, by the relationship of vehicle speed and the position of discrete wind velocity point.

D. Wind Loads on the Vehicle

To investigate the whole process of vehicles entering and leaving the wind barrier section under the strong wind circumstance, the wind barriers were positioned at the middle section of the 20-span bridge from the 7th to the 13th bridge. The distribution of the wind barriers on the bridge can be seen in Fig. 5. According to the aerodynamic characteristics of vehicles corresponding to the different wind barrier types from Table I, the wind loads on the vehicle at the different position can be obtained.

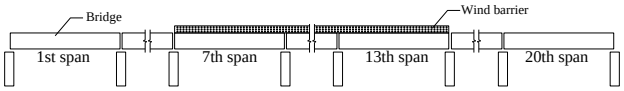

Figure 5. Distribution of the wind barriers on the bridge.

IV. DY NAMIC RESPONSES OF VEHICLE

A. Effects of Vehicle Speeds

The 43.5% porosity was adopted for the wind barriers, and the dynamic responses of vehicle at different operating speeds were listed in Table II.

TABLE II. DYNAMIC RESPONSES OF VEHICLE AT DIFFERENT OPERATING SPEEDS

	Vehicle speed (km/h)				
	150	175	200	225	250
Lateral acceleration (m/s^2)	0.831	0.935	0.914	0.952	1.331
Vertical acceleration (m/s^2)	0.790	0.808	0.883	0.741	0.927
Lateral force (kN)	20.30	21.68	23.02	22.13	30.72
Reduction rate of wheel load	0.501	0.525	0.586	0.587	0.683
Derailment coefficient	0.161	0.169	0.199	0.182	0.244
Lateral Sperling index	2.082	2.172	2.285	2.372	2.558
Vertical Sperling index	1.929	1.877	1.934	2.023	2.112

From Table I, static aerodynamic coefficients of the vehicle with wind barriers of 100% porosity and of 43.5% porosity are greatly changed, in which drag coefficient varies largest. Therefore, the vehicle is subjected to a sudden change when entering and leaving the wind barrier section. With the 43.5% porosity of wind barrier, the time histories of dynamic responses of vehicle at vehicle operating speeds of 150, 200 and 250km/h are shown in Figs. 6~9.

In general, the responses of the vehicle tend to increase with the increase in speed. And in the wind barrier section, the dynamic responses would decrease, accounting for the wind shielding effects.

The sudden change of wind loads on the vehicle has great effects on lateral and vertical accelerations. With

the vehicle speed increasing, the sudden change becomes more obvious.

The wind loads is dominant in lateral force and reduction rate of wheel load. In wind barrier section, the lateral force and reduction rate of wheel load tend to be decrease, accounting for the wind shielding effects of wind barriers. However, the sudden change is not evident for these two responses.

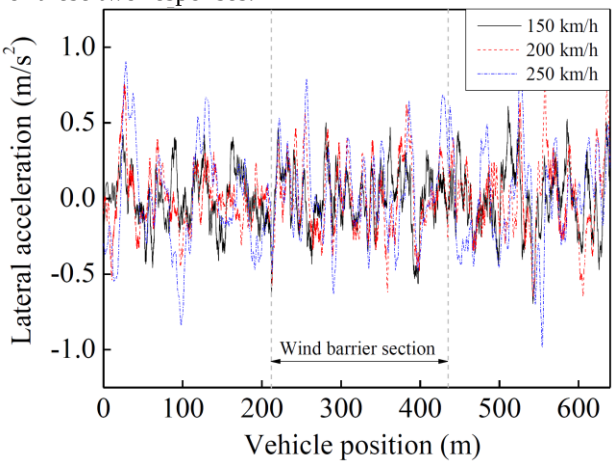

Figure 6. Time histories of lateral acceleration.

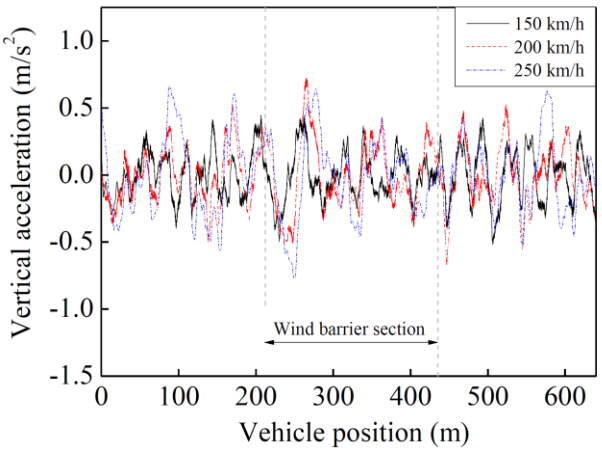

Figure 7. Time histories of vertical acceleration.

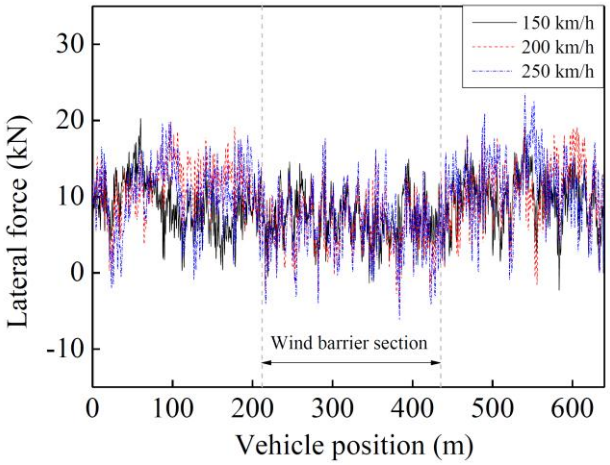

Figure 8. Time histories of lateral force.

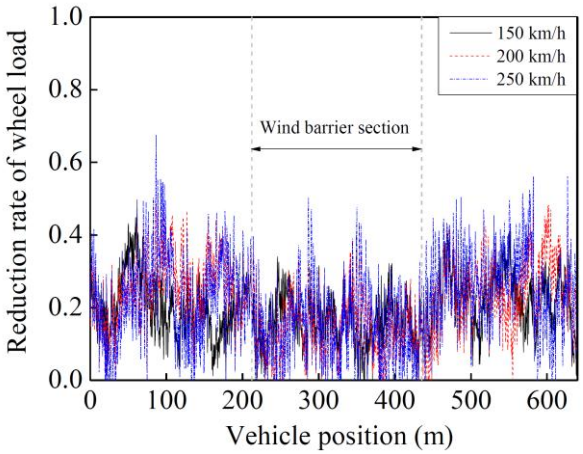

Figure 9. Time histories of reduction rate of wheel load.

B. *Effects of Wind Barrier Porosities*

Three porosities of wind barriers were compared, i.e. 100%, 43.5% and 0%. The vehicle speed was set as 250 km/h. The dynamic responses of vehicle with different porosities of wind barriers on the bridge were listed in Table III.

TABLE III. DYNAMIC RESPONSES OF VEHICLE AT DIFFERENT WIND BARRIER POROSITIES

	Wind barrier porisity		
	100%	43.5%	0%
Lateral acceleration (m/s²)	1.306	1.331	1.436
Vertical acceleration (m/s²)	0.927	0.927	1.036
Lateral force (kN)	30.44	30.72	30.48
Reduction rate of wheel load	0.683	0.683	0.683
Derailment coefficient	0.240	0.244	0.247
Lateral Sperling index	2.557	2.558	2.592
Vertical Sperling index	2.126	2.112	2.210

The time histories of dynamic responses of vehicle with different porosities of wind barriers on the bridge are shown in Figs. 10~13.

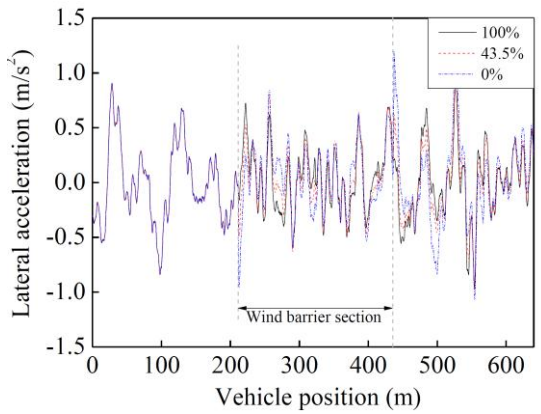

Figure 10. Time histories of lateral acceleration.

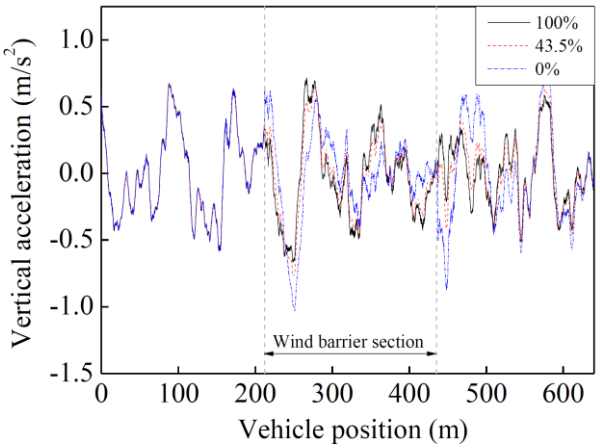

Figure 11. Time histories of vertical acceleration.

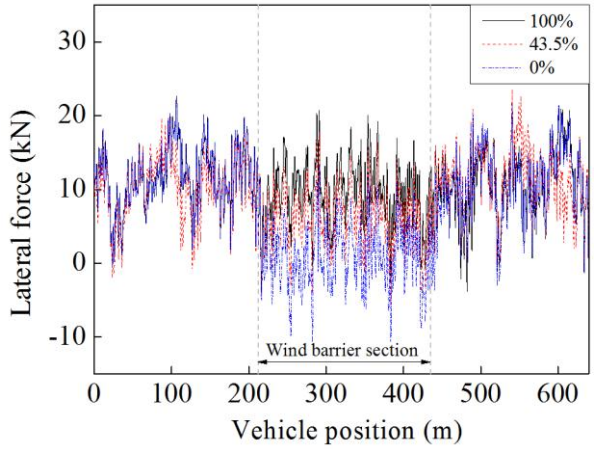

Figure 12. Time histories of lateral force.

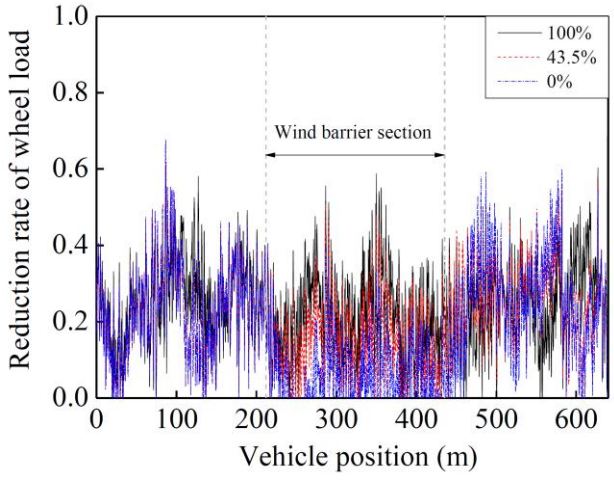

Figure 13. Time histories of reduction rate of wheel load.

The lateral and vertical accelerations with the wind barriers of 0% porosity are larger than other situations. It can be seen that when the vehicle enters or leaves the wind barrier section, the lateral and vertical accelerations have sudden changes, which is demonstrates that the accelerations are sensitive to the sudden changes of wind loads.

As for the lateral force and reduction rate of wheel load, the two responses are mainly influenced by the wind loads. Hence, with the decrease of wind barrier porosity, the lateral force and reduction rate of wheel load decrease apparently. And the sudden change is not evident for these two responses as well.

V. Conclusions

(1) Static aerodynamic coefficients of the vehicle have great differences considering different wind barrier porosities, in which drag coefficient varies largest.

(2) The dynamic responses of the vehicle generally tend to increase with the increase in speed. In the wind barrier section, the dynamic responses would decrease, accounting for the wind shielding effects.

(3) The lateral and vertical accelerations are sensitive to the sudden changes of wind loads. With the increase of the vehicle speed and decrease of the wind barrier porosity, the sudden change becomes more obvious.

(4) The lateral force and reduction rate of wheel load are mainly affected by the wind loads, and the sudden change of wind loads would not lead to the sudden change of the two responses. In addition, with the decrease of wind barrier porosity, the lateral force and reduction rate of wheel load would decline apparently for the wind shielding effects of wind barriers.

Acknowledgment

This work was supported in part by a grant from China Railway Eryuan Engineering Group Co., Ltd. and the National Key R&D Program of China (2017YFB1201204).

References

[1] T. Johnson. "Strong wind effects on railway operation - 16th October 1987," *Journal of Wind Engineering and Industrial Aerodynamics*, vol. 60, pp. 251-266, April 1996.

[2] T. Fujii, T. Maeda, H. Ishida, T. Imai, K. Tanemoto, and M. Suzuki. "Wind-induced accidents of train/vehicles and their measures in Japan," *Quarterly Report of RTRI*, vol. 40: pp: 50-55, January 1999.

[3] C. Baker, F. Cheli, A. Orellana, N. Paradot, C. Proppe, and D. Rocchi. "Cross-wind effects on road and rail vehicles," *Vehicle System Dynamics*, vol. 47, pp. 983-1022, August 2009.

[4] C. R. Chu, C. Y. Chang, C. J. Huang, T. R. Wu, C. Y. Wang, and M. Y. Liu. "Windbreak protection for road vehicles against crosswind," *Journal of Wind Engineering and Industrial Aerodynamics*, vol. 116, pp. 61-69, May 2013.

[5] M. Ogueta-Guti érrez, S. Franchini, and G. Alonso. "Effects of bird protection barriers on the aerodynamic and aeroelastic behaviour of high speed train bridges," *Engineering Structures*, vol. 81, pp. 22-34, December 2014.

[6] H. Y. Xiang, Y. L. Li, and B. Wang. "Aerodynamic interaction between static vehicles and wind barriers on railway bridges exposed to crosswinds," *Wind and Structures*, vol. 20, pp. 237-247, February 2015.

[7] H. Y. Xiang, Y. L. Li, S. R. Chen, and G. Y. Hou. "Wind loads of moving vehicle on bridge with solid wind barrier," *Engineering Structures*, vol. 156, pp. 188-196, February 2018.

[8] R. H. Scanlan and N. P. Jones. "Aeroelastic analysis of cable-stayed bridges," *Journal of Structural Engineering*, vol. 116, pp. 279-297, February 1990.

[9] Y. L. Li, S. Z. Qiang, H. L. Liao, and Y. L. Xu. "Dynamics of wind-rail vehicle-bridge systems," *Journal of Wind Engineering and Industrial Aerodynamics*, vol. 93, pp. 483-507, June 2005.
[10] X. Y. Xu and Y. L. Li. "Dynamic analysis of wind-vehicle-bridge system based on rigid-flexible coupling method," presented at 2016 World Congress on Advances in Civil, Environmental and Materials Research (ACEM16) / 2016 Structures Congress (Structures16), Jeju Island, Korea, August 28- September 1, 2016.
[11] Y. L. Li, X. Y. Xu, Y. Zhou, C. S. Cai, and J. X. Qin. "An interactive method for the analysis of the simulation of vehicle–bridge coupling vibration using ANSYS and SIMPACK," *Proceedings of the Institution of Mechanical Engineers, Part F: Journal of Rail and Rapid Transit*, vol. 232, pp. 663-679, March 2018.
[12] X. Y. Xu. "Coupling Vibration of wind-rail vehicle-bridge system in complex mountainous terrain," Ph.D. dissertation, Dept. Bridge Eng., Southwest Jiaotong Univ., Chengdu, China, 2017.

Xu Xinyu was born in China. He received his doctor degree of bridge and tunnel engineering from Southwest Jiaotong University in 2017. His major field of study: bridge wind engineering and vehicle-bridge vibration. He is working for China Railway Eryuan Engineering Group Co., Ltd.

Zheng Xiaolong was born in China. He graduated from Sichuan University in 1997. He is working for China Railway Eryuan Engineering Group Co., Ltd. as professorate senior engineer. Current and previous research interests are bridge design, dynamics of bridge and train-bridge coupling vibration.

Li Yongle was born in China. He received his doctor degree of bridge and tunnel engineering from Southwest Jiaotong University in 2003. His major field of study: bridge wind engineering and vehicle-bridge vibration. He is working for Southwest Jiaotong University as professor.